Chinese Journal of Chemistry, **2004**, *22*, 243—251 **Article**

Theoretical Studies on the Third-order Nonlinear Optical Properties and Two-photon Absorption of Stilbene Derivatives

REN, Ai-Min[a](任爱民) FENG, Ji-Kang*[,a,b](封继康) LIU, Xiao-Juan[a](刘孝娟)

[a] *State Key Laboratory of Theoretical and Computational Chemistry, Institute of Theoretical Chemistry , Jilin University, Changchun, Jilin 130023, China*

[b] *College of Chemistry, Jilin University, Changchun, Jilin 130023, China*

Different types of stilbene derivatives (D-π-D, A-π-A, D-π-A) were investigated with AM1, and specially, equilibrium geometries of symmetrical stilbene derivatives (D-π-D) were studied using of PM3. With the same method INDO/CI, the UV-vis spectra were explored and the position and strength of the two-photon absorption were predicated by Sum-Over-States expression. The relationships of the structures, spectra and nonlinear optical properties have been examined. The influence of various substituents on two photon absorption cross-sections was discussed micromechanically.

Keywords stilbene derivative, electronic spectrum, two-photon absorption cross-section

Introduction

Two-photon absorption (TPA) was theoretically predicated[1] by Matis Göppert-Mayer in 1931 and firstly observed[2] by Kaiser and Garret in a $CaF_2:Eu^{2+}$ crystal, shortly after the advent of lasers. TPA is a third-order nonlinear optical (NLO) process in which an atom or a molecule can simultaneously absorb two photons and the transition probability for absorption of two identical photons is proportional to I^2, where I is the intensity of the incident radiation. For several decades there has been extensive research in the area of two-photon spectroscopy. However, TPA has not found widespread application due to the relative low TPA cross sections (δ) for most materials. Recently, some novel organic compounds were found to have unprecedented δ values and have been applied in many areas.[3-14] A systematic study of the relationship between the structure of a molecule and its TPA property is necessary to design new molecules with enhanced TPA at a desired wavelength.

Stilbene-like compounds have been studied for many years because of their important role in the field of chemical physics. During the past years, numerous experimental and theoretical studies have focused on the nonlinear optical properties of donor-acceptor conjugated molecules,[15,16] which possess easily polarizable electron clouds and asymmetric charge distributions. The charge transfer occurring in the donor-conjugated bridge-acceptor systems can lead to significant enhancement of the NLO response.

Recently, symmetrically substituted with donor groups conjugated systems[17] were reported to have strong TPA and have attracted considerable interests. In order to gain insight into the origin of the large δ values for this type of molecules, in the first section we design a series of symmetrically substituted with donor groups stilbene (D-π-D) and performed quantum chemical calculations on them.

Study of D-π-D type derivatives stimulates us go on to step into the A-π-A [two same acceptor (A) groups are connected via a π-conjugated system], D-π-A [donor (D) and acceptor (A) groups are connected via a π-conjugated system] type molecules. So in the second section, we designed three types of stilbene derivatives (D-π-D, A-π-A and D-π-A) and discussed them micromechanically, at the same time compared them systematically. All we have done was to provide theoretical basis for the synthesis.

Methodology

TPA cross-section δ is related to the imaginary part of the third-order polarizability $\gamma(-\omega;-\omega,\omega,\omega)$ by the expression[18]

$$\delta = \frac{8\pi^2\hbar\omega^2}{n^2c^2}\,\mathrm{Im}\,\gamma(-\omega;\omega,\omega,-\omega) \qquad (1)$$

where $\hbar$ is Plank's constant divided by 2π; $\omega/2\pi$ is photon frequency, c is the speed of light and n is the refractive index of the medium, Im means to take imaginary part of the variant.

The sum-over-states (SOS) expression to evaluate the components of the third-order polarizability γ_{ijkl} can

* E-mail: jikangf@yahoo.com

Received May 6, 2003; revised September 22, 2003; accepted November 3, 2003.
Project supported by the National Natural Science Foundation of China (Nos. 20273023, 90101026) and the Key Laboratory for Supramolecular Structure and Material of Jilin University.

$$\gamma_{ijkl}(-\omega_\sigma;\omega_1,\omega_2,\omega_3)=\frac{4\pi^3}{3h^3}P(i,j,k,l;-\omega_\sigma;\omega_1,\omega_2,\omega_3)\left[\sum_{m\neq o}\sum_{n\neq o}\sum_{p\neq o}\frac{\langle o|\mu_i|m\rangle\langle m|\bar{\mu}_j|n\rangle\langle n|\bar{\mu}_k|p\rangle\langle p|\mu_l|o\rangle}{(\omega_{mo}-\omega_\sigma-i\Gamma_{mo})(\omega_{no}-\omega_2-\omega_3-i\Gamma_{no})(\omega_{po}-\omega_3-i\Gamma_{po})}-\sum_{m\neq o}\sum_{n\neq o}\frac{\langle o|\mu_i|m\rangle\langle m|\mu_j|o\rangle\langle o|\mu_k|n\rangle\langle n|\mu_l|o\rangle}{(\omega_{mo}-\omega_\sigma-i\Gamma_{mo})(\omega_{no}-\omega_3-i\Gamma_{no})(\omega_{no}+\omega_2-i\Gamma_{no})}\right] \quad (2)$$

be induced out using perturbation theory and density matrix method. By considering a power expansion of the energy with respect to the applied field, the γ_{ijkl} Cartesian components are given by Eq. (2).[19] where $P(i,j,k,l;-\omega_\sigma;\omega_1,\omega_2,\omega_3)$ is a permutation operator defined in such a way that for any permutation of (i, j, k, l), an equivalent permutation of $(-\omega_\sigma; \omega_1, \omega_2, \omega_3)$ is made simultaneously; $\omega_\sigma=\omega_1+\omega_2+\omega_3$ is the polarization response frequency; ω_1, ω_2 and ω_3 indicate the frequencies of the perturbing radiation fields (considering the degenerate TPA, $\omega_1=-\omega$ and $\omega_2=\omega_3=\omega$) ; *i*, *j*, *k* and *l* correspond to the molecular axes *x*, *y* and *z*; *m*, *n* and *p* denote excited states and *o*, the ground state; μ_i is the *j*th$(=x,y,z)$ component of the dipole operator $(\langle m|\bar{\mu}_j|n\rangle=\langle m|\mu_j|n\rangle-\langle o|\mu_j|o\rangle)$; $(h/2\pi)\omega_{mo}$ is the transition energy between the *m* and *o* states, and Γ_{mo} is the damping factor of excited state *m*. We consider that the higher the excited state the shorter its lifetime is, and express the damping , in eV, as

$$\Gamma_{mo}=0.10\times\frac{\omega_{mo}}{\omega_{1o}}$$

Up to now, TPA has remained difficult to characterize quantitatively due to the resonance nature of this process.[15,20,21] Here the position and relative strength of the two-photon resonance for a series of stilbene derivatives are to be predicated using the following simplified form of the SOS expression:[15,21]

$$\delta\propto\frac{M_{01}^2M_{1n}^2}{\left(E_{01}-E_{1n}/2\right)^2} \quad (3)$$

where M_{ij} is the transition dipole moment from the state *i* to *j*, E_{ij} is the corresponding excitation energy, the subscripts 0, 1 and *n* refer to the ground state S_0, the first excited state S_1 and the TPA final state S_n, respectively. This expression results from taking S_1 as the dominant intermediate state and is valid when $(E_{01}-\hbar\omega)$ is large compared with the damping factor for the $S_0\rightarrow S_1$ transition.

In principle, any kind of self-consistent field molecular orbital (SCFMO) procedure combined with configuration interaction (CI) can be used to calculate the physical values in the above expression. In this paper, the semi-empirical-intermediate neglect of differential overlap (INDO) formalism[22] was firstly used to calculate molecular orbital. Then, the molecular electronic structure was obtained by configuration interaction (CI). Furthermore, either UV-vis (ground-state one-photon absorption) spectra or the transition dipole moment and the corresponding transition energy which were needed to predict TPA were provided. The position and relative strength of the TPA for a series of stilbene derivatives were to be predicated by Eq. (3), and the exact values of TPA cross-section δ were to be obtained by Eq. (1) combined with SOS Eq. (2). All these computations were performed on the equilibrium geometry optimized using PM3/AM1 method respectively.

Results and discussion

Symmetrical D-π-D stilbene derivatives

Structural design and geometry optimization

The third-order nonlinear optical effect of organic conjugated systems arises from the delocalization of their π electrons. On the basis of the compounds reported by the literaure[17], we designed a series of symmetrically substituted stilbene derivatives D-π-D at first that is to say compounds **1**—**6** (following called series I for short, as shown in Figure 1) considering the importance of the substitution effect and the different donor-electron capabilities of alkyl, amino and phenyl. They each have a center of inversion symmetry in the chemical structure.

Full geometry optimizations were carried out using the PM3 semi-empirical Hamiltonian. For every compound studied in this paper, the two phenyl rings in the middle are almost in the same plane. The planar structures can safely be employed in the spectroscopic studies on stilbene-like systems, which has been supported by a lot of theoretical and experimental works.[23] The main bond distances and a few selected bond angles are listed in Table 1 and the corresponding atom labels are shown in Figure 2.

Electronic structure for series I On the basis of the equilibrium geometry, the electronic structure was calcualted using INDO method in the ZINDO program. The highest occupied molecular orbital (HOMO) and the lowest unoccupied molecular orbital (LUMO) distribution diagrams for compounds **1**—**6** are depicted in Figure 3.

With the molecule placed in the *xy* plane, the main contributions to the conjugation effect is due to the $2p_z$ atomic orbitals, which is confirmed by our results. According to the atom labels in Figure 2, the π molecular

orbital wave function can be given by

$$\Psi_{MO} = \cdots + \alpha 8\Phi_{p_z}(8) + \alpha 7\Phi_{p_z}(7) + \alpha 6\Phi_{p_z}(6) + \alpha 5\Phi_{p_z}(5) + 4\Phi_{p_z}(4) + \alpha 3\Phi_{p_z}(3) + \alpha 2\Phi_{p_z}(2) + \alpha 1\Phi_{p_z}(1) + \alpha 1'\Phi_{p_z}(1') + \alpha 2'\Phi_{p_z}(2') + \alpha 3'\Phi_{p_z}(3') + \alpha 4'\Phi_{p_z}(4') + \alpha 5'\Phi_{p_z}(5') + \alpha 6'\Phi_{p_z}(6') + \alpha 7'\Phi_{p_z}(7') + \alpha 8'\Phi_{p_z}(8') + \cdots \quad (4)$$

where $\alpha 8$, ⋯, $\alpha 8'$ are atomic orbital coefficient. The main composition of the HOMO and LUMO are compiled in Table 2.

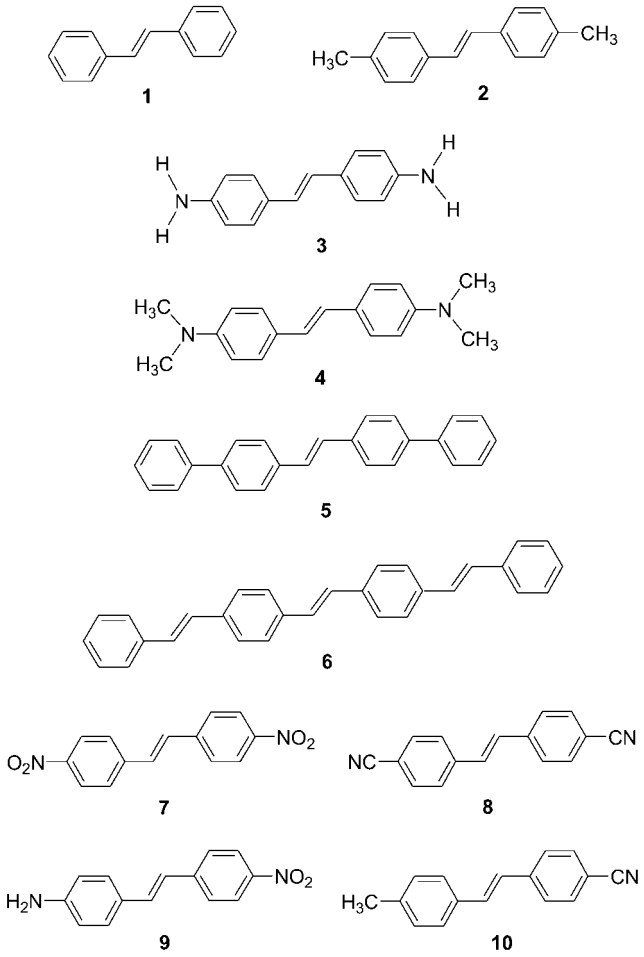

Figure 1 Structures and numbering scheme for three type stilbene derivatives.

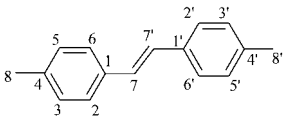

Figure 2 Atom labeling scheme for molecules studied in this paper.

One- and two-photon absorption for series I By singly exciting all electrons in the highest 14 molecular orbitals to the lowest 14 virtual molecular orbi tals, 196 excited configurations with respect to the ground state configuration were firstly generated, then we obtained 196 excited states by CI method. Furthermore, the vertical transition energies and oscillator strengths from the ground state to each excited state were calculated, giving the UV-vis spectrum. The calculated wavelength λ_{1c}, oscillator strength f and transition nature (configurations and weight) for the maximum one-photon absorption (OPA) are shown in Table 3 and the corresponding experimental values λ_{1e} are given in parentheses. The calculated results are basically in agreement with the experimental values and both are successively red-shifted from compound **1** to **6** (red-shifted from compound **1** to **3** and **4** for experimental values). It can be seen from the transition nature, that the most intense OPA peaks for compounds **1**—**6** all correspond to the transition to the excited states with

Table 1 Geometrical parameters for the compounds **1**—**6** from PM3 geometry optimizations [bond distance *r*/nm, bond angle *θ*/(°)]

Parameter	**1**	**2**	**3**	**4**	**5**	**6**
r(7)(7')	1.344	1.345	1.345	1.344	1.343	1.343
r(1)(7)[a] *r*(1')(7')	1.453	1.450	1.450	1.452	1.456	1.456
r(1)(2)[a] *r*(1')(2')	1.407	1.405	1.406	1.406	1.399	1.400
r(2)(3)[a] *r*(2')(3')	1.391	1.386	1.385	1.391	1.387	1.387
r(3)(4)[a] *r*(3')(4')	1.396	1.419	1.419	1.400	1.400	1.400
r(4)(5)[a] *r*(4')(5')	1.393	1.418	1.417	1.400	1.400	1.400
r(5)(6)[a] *r*(5')(6')	1.394	1.388	1.387	1.382	1.386	1.386
r(1)(6)[a] *r*(1')(6')	1.402	1.401	1.402	1.403	1.399	1.399
θ(1)(7)(7')[a] *θ*(1')(7')(7)	125.3	125.5	125.5	125.4	123.1	123.1
θ(2)(1)(7)[a] *θ*(2')(1')(7')	118.5	119.1	118.9	118.7	119.8	119.8
θ(6)(1)(7)[a] *θ*(6')(1')(7')	122.8	123.1	123.1	122.9	121.2	121.1

[a] The bond distances and bond angles at symmetrically position are equal.

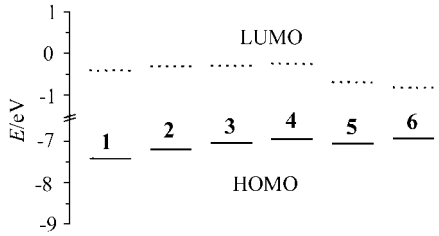

Figure 3 Schematic diagram showing the HOMO and LUMO distribution of compounds **1**—**6**.

Table 2 Main composition of the HOMO and LUMO for compounds **1**—**6**

Compound	MO	$\alpha1$ ($\alpha1'$)	$\alpha2$ ($\alpha2'$)	$\alpha3$ ($\alpha3'$)	$\alpha4$ ($\alpha4'$)	$\alpha5$ ($\alpha5'$)	$\alpha6$ ($\alpha6'$)	$\alpha7$ ($\alpha7'$)	$\alpha8$ ($\alpha8'$)
1	LUMO	−0.28 (0.28)	0.25 (−0.25)	0.11 (−0.11)	−0.32 (0.32)	0.10 (−0.10)	0.26 (−0.26)	−0.41 (−0.41)	
	HOMO	0.28 (0.28)	0.25 (0.25)	−0.11 (−0.11)	−0.32 (−0.32)	−0.10 (−0.10)	0.26 (0.26)	−0.41 (−0.41)	
2	LUMO	0.26 (−0.26)	−0.25 (0.26)	−0.09 (0.07)	0.33 (−0.33)	−0.07 (0.09)	−0.26 (0.25)	−0.41 (0.41)	−0.13 (0.13)
	HOMO	0.29 (0.29)	0.20 (0.20)	−0.18 (−0.18)	−0.26 (−0.26)	−0.18 (−0.18)	0.20 (0.20)	−0.32 (−0.32)	0.30 (0.30)
3	LUMO	−0.26 (0.26)	0.25 (−0.26)	0.07 (−0.08)	−0.33 (0.33)	0.07 (−0.09)	0.26 (−0.25)	−0.41 (0.41)	0.13 (−0.13)
	HOMO	0.29 (0.29)	0.21 (0.21)	−0.18 (−0.18)	−0.29 (−0.29)	−0.18 (−0.18)	0.21 (0.21)	−0.34 (−0.34)	0.26 (0.26)
4	LUMO	−0.27 (0.27)	0.25 (−0.25)	0.10 (−0.09)	−0.33 (0.33)	0.09 (−0.10)	0.25 (−0.25)	−0.41 (0.41)	0.02 (−0.02)
	HOMO	0.29 (0.29)	0.25 (0.24)	−0.13 (−0.13)	−0.32 (−0.32)	−0.14 (−0.13)	0.24 (0.25)	−0.39 (−0.39)	0.06 (0.06)
5	LUMO	−0.27 (0.27)	0.20 (−0.20)	0.14 (−0.14)	−0.30 (0.30)	0.14 (−0.14)	0.21 (−0.21)	−0.34 (0.34)	−0.15 (0.15)
	HOMO	0.27 (0.27)	0.21 (0.21)	−0.14 (−0.14)	−0.30 (−0.30)	−0.14 (−0.14)	0.21 (0.21)	−0.33 (−0.33)	0.15 (0.15)
6	LUMO	0.25 (−0.25)	−0.18 (0.18)	−0.15 (0.15)	0.27 (−0.27)	−0.14 (0.14)	−0.18 (0.18)	0.30 (−0.30)	0.19 (−0.19)
	LUMO	−0.25 (−0.25)	−0.18 (−0.18)	0.15 (0.15)	0.27 (0.27)	0.15 (0.15)	−0.19 (−0.19)	0.29 (0.29)	−0.18 (−0.18)

Table 3 Maximum one- and two-photon absorption for compounds of series I

Compound	λ_{1c} (λ_{1e})[a]/nm	f	Configurations and weight	λ_{2c} (λ_{2e})[a]/nm	Configurations and weight
1	330.96 (312[24])	1.0168	(34,0)→(35,0) 94% (34,0)→(36,0) 2%	475 (488[25]), (466[21])	(31,0)→(35,0) 67% (32,0)→(35,0) 10%
2	338.85	1.0257	(40,0)→(41,0) 91% (40,0)→(42,0) 4%	490	(39,0)→(41,0) 84% (38,0)→(43,0) 4%
3	350.04 (348[26])	1.1151	(40,0)→(41,0) 91% (40,0)→(42,0) 3%	513	(39,0)→(41,0) 81% (40,0)→(44,0) 5%
4	352.94 (364[26])	1.1721	(52,0)→(53,0) 92% (51,0)→(56,0) 3%	522 (529[21])	(51,0)→(53,0) 64% (52,0)→(56,0) 22%
5	375.05	1.8887	(62,0)→(63,0) 88% (61,0)→(64,0) 8%	543	(61,0)→(63,0) 56% (62,0)→(64,0) 20%
6	398.24	2.4223	(72,0)→(73,0) 81% (71,0)→(74,0) 13%	570	(71,0)→(73,0) 43% (72,0)→(74,0) 24%

[a] The experimental values λ_{1e} and λ_{1e} are given in parentheses.

odd parity, which are described mainly by the one-electron promotion from the HOMO to the LUMO (Table 2, the symmetries of the HOMO and the LUMO are different) and are dipole-allowed.

The absorption of light by matter is a consequence of the interaction of an electromagnetic field with optically induced electric dipoles in a molecule. A change in the parity between the initial and final states (wave functions) is required for every photon involved in the transition for electronic dipole transitions. Thus the selec-

tion rule for TPA is different from that of OPA.[18] One change of parity is required for an one-photon transition, while two-photon transitions must have initial and final states with the same parity.

First, In this paper, the transition staring from the ground state (typically an even symmetry state A_g) are concerned, therefore the TPA only allows the even parity excited states A_g to be identified. Second, from Eq. (3), it can be seen that the TPA cross-section δ is related to the transition dipole moments M_{01}, M_{1n} and the corresponding transition energy E_{01}, E_{1n}. According to the above two limits, the S_5, S_7 and S_8 were regarded as the final states of TPA for compounds **1**—**4**, **5** and **6** respectively. The wavelength λ_{2c} of the TPA peaks for compounds **1**—**6** are listed in Table 3.

The calculated transition dipole moments (in Debye), the vertical transition energies (in electron volt) and the TPA cross section δ [calculated from Eqs. (1) and (2) are listed in Table 4]. The experimental values λ_{2e} and δ of stilbene are given in parentheses, and is in good agreement with our calculated result.

To conclude, there are shifts of the one- and two-photon absorption peaks to longer wavelength and increase of δ from the compound **1** to **6**. For compound **2**, the substitution of alkyl has only a small effect to the position and strength of one- and two-photon absorption and TPA cross section δ; For compounds **3** and **4**, the changes resulting from the substitution of NR_2 are clear, which can be interpreted as the introduction of p-π conjugation by p orbital of nitrogen atom, which change the distribution and composition of π and π* molecular orbitals. For compounds **5** and **6**, the conjugation length was increased by attaching phenyl or phenethyl groups on both ends, which enlarge the extent of electronic delocalization and facilitate the conjugation effect.

Different type stilbene derivatives

Above are the D-π-D type stilbene derivatives, some other groups also studied them both on theoretical and experimental methods recently[21], but systematic studies for the D-π-A, A-π-A type stilbene derivatives are rare to the best of our knowledge. D-π-A, A-π-A molecules constitute the important class of NLO chromophores. Here, three different types of stilbene derivatives (D-π-D D-π-A, A-π-A), type D-π-D just the same as series I are designed, and their equilibrium structures, electronic spectra, compared with experimental data are studied. On this base, their third-order polarizabilities (γ) and two-photon absorption cross-sections (δ) are explored, bringing the effect of different structures on γ and δ to light. By the way, AM1 was used to get the equilibrium structure in series II. It is significant to compare the two different geometry optimized methods (AM1 and PM3) for study the effect of geometry to third-order polarizabilities (γ) and two-photon absorption cross-sections (δ).

Structural design and geometry optimization We designed 8 stilbene derivatives (they are molecules **1**—**4** and **7**—**10** shown in Figure 1, following called series II for short), belonging to three different types. Here **2**, **3**, **4** belong to D-π-D type, **7** and **8** A-π-A type, **9** and **10** D-π-A type.

Full geometry optimizations were carried out using AM1 method. Some bond distances and some bond angles for **1**—**4** and **7**—**10** are shown in Table 5.

Electronic structure for series II On the basis of the AM1 equilibrium geometry, we calculated the electronic structure using INDO method in the ZINDO program. The highest occupied molecular orbital (HOMO) and the lowest unoccupied molecular orbital (LUMO) distribution diagrams for molecules **1**—**4** and **7**—**10** are depicted in Figure 4.

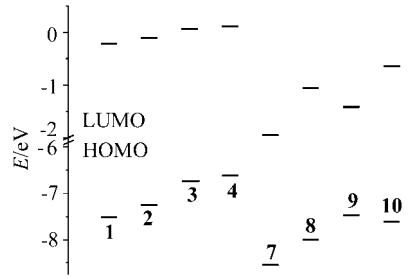

Figure 4 Schematic diagram showing the HOMO and LUMO distribution of molecules **1**—**4** and **7**—**10**.

According to the same atom labels (Figure 2) and Eq. (4), the main composition of the HOMO and LUMO are compiled in Table 6.

In order to compare the effect of the different structure on the delocalization, it is necessary to study the charge distribution. According to Figure 2, we select the charge distribution of substitutes at position 8 (8') as our

Table 4 Calculated transition dipole moments, vertical transition energies and cross section δ for TPA

Compound	Final state	M_{01}/D	M_{1n}/D	E_{01}/eV	E_{1n}/eV	$M_{01}^2 M_{1n}^2 \left(E_{01}-E_{1n}/2\right)^{-2}$	$\delta(\omega)\times10^{-50}$/(cm^4·s)
1	5	8.45	8.07	3.75	1.48	902.42	27.02(12[a]) [21]
2	5	8.59	9.47	3.67	1.40	1284.21	29.74
3	5	9.10	12.43	3.55	1.29	2505.00	33.51
4	5	9.37	13.96	3.52	1.24	3291.40	33.83
5	7	12.27	16.07	3.31	1.27	9342.44	76.44
6	8	14.31	17.51	3.12	1.24	17763.80	179.76

[a] The experimental value δ is given in parentheses.

Table 5 Geometrical parameter for compounds **1**—**4**, **7**—**10** from AM1 geometry optimizations methods [bond distances in 0.1 nm and bond angles in (°)]

Parameter	**1**	**2**	**3**	**4**	**7**	**8**	**9**	**10**
r(7)(7')	1.344	1.344	1.345	1.345	1.344	1.344	1.346	1.344
r(1)(7)[a]	1.453	1.452	1.450	1.450	1.454	1.453	1.448	1.452
r(1')(7')							1.450	1.452
r(1)(2)[a]	1.407	1.406	1.406	1.405	1.406	1.406	1.407	1.406
r(1')(2')							1.404	1.403
r(2)(3)[a]	1.391	1.391	1.385	1.386	1.390	1.396	1.384	1.391
r(2')(3')							1.391	1.392
r(3)(4)[a]	1.396	1.400	1.419	1.419	1.404	1.404	1.420	1.403
r(3')(4')							1.404	1.400
r(4)(5)[a]	1.393	1.400	1.417	1.418	1.404	1.400	1.419	1.402
r(4')(5')							1.406	1.400
r(5)(6)[a]	1.394	1.382	1.387	1.388	1.391	1.389	1.386	1.392
r(5')(6')							1.388	1.391
r(1)(6)[a]	1.402	1.403	1.402	1.401	1.403	1.401	1.403	1.404
r(1')(6')							1.408	1.406
θ (1)(7)(7')[a]	125.3	125.4	125.5	125.5	125.2	125.3	125.5	125.3
θ (1')(7')(7)							125.2	125.3
θ (2)(1)(7)[a]	118.5	118.7	118.9	119.1	118.2	118.6	118.8	118.6
θ (2')(1')(7')							122.8	122.8
θ (6)(1)(7)[a]	122.8	122.9	123.1	123.1	122.7	121.7	123.1	122.7
θ (6')(1')(7')							118.5	118.6

[a] The bond distances and bond angles at symmetrically position are equal.

studied subject, q_0 denoting the charge distribution of ground state and q_s , excited state. Plus the change of the charge (Δq) between the ground and excited state they are shown in Table 7, It is obvious that: (1) For the substitutes of H, CH_3, NH_2, $N(CH_3)_2$, the change of the charge quantity is positive, telling that they are donors (D), what's more, from Δq**1**$<\Delta q$**2**$<\Delta q$**3**$<\Delta q$**4**, we can say that the donating ability of the substitutes is: H$<$ $CH_3<NH_2<N(CH_3)_2$. (2) To the substitutes of CN, NO_2 the change is negative, showing that they are acceptors (A), and Δq**8**$<\Delta q$**7**, we know that the accepting ability is: CN$<NO_2$. (3) The molecules **7** and **8** are D-π-A type compounds, from the table, we can conclude that no matter what is the donor (NH_2, CH_3) and the acceptor (CN, NO_2), the change of the charge quantity is larger than that of the first two type (D-π-D and A-π-A) molecules, indicating that D-π-A type of molecules can facilitate delocalization.

One and two-photon absorption Using the same methods, the one-photon absorption was calculated, and the results were listed in Table 8, basically in agreement with the experiment. We can easily conclude that with the accepting or donating ability increase, λ_{1c} has a red-shift. That's to say: for the D-π-D type, the value of λ_{1c} progressively increase in H, CH_3, NH_2, $N(CH_3)_2$ order; while for the A-π-A type molecules, the value of λ_{1c} successively increase in CN, NO_2 order, and for D-π-A type ones, the value connecting with CH_3 and CN is smaller than the one connecting with NO_2 and NH_2. From the transition nature, we can find out that for molecules **1**—**4** and **7**—**8**, the strongest peaks of OPA correspond to the transition to the excited state with odd parity, which are described mainly by the single electronic transition from HOMO to LUMO (refer to the Table 6, the symmetry of HOMO and LUMO are different). Furthermore, these transitions are dipole-allowed.

To position the peak of TPA, we have this process divided into three steps: (1) The determination of the molecular symmetry. On the basis of calculation, one case is that the molecule has central symmetry, which must have the same parity of their TPA transition starting from ground state to the final state (as **1**—**4** and **7**—**8**); the other case is molecule without a center of inversion symmetry, every state is of mixed parity and hence transitions between all electronic states involving any number of photons are allowed (such as **9**, **10**). So on principle there is no symmetry limits on the ground and excited states of the one and two-photon transition. (2) The determination of the middle state. For the molecules **1**—**4**, **8**, **10** their strongest peaks are caused by the transition $S_0 \rightarrow S_1$, then the main middle state is S_1, while whose of **7** and **9** are caused by the transition $S_0 \rightarrow S_5$, $S_0 \rightarrow S_2$ respectively, so the main middle states are S_5 and S_2. (3) On the basis of steps 1 and 2, during the

Table 6 Main composition of the HOMO and LUMO for molecules **1**—**4** and **7**—**8**

Compound	MO	$\alpha1$ ($\alpha1'$)	$\alpha2$ ($\alpha2'$)	$\alpha3$ ($\alpha3'$)	$\alpha4$ ($\alpha4'$)	$\alpha5$ ($\alpha5'$)	$\alpha6$ ($\alpha6'$)	$\alpha7$ ($\alpha7'$)	$\alpha8$ ($\alpha8'$)
1	LUMO	−0.28 (0.28)	0.25 (−0.25)	0.11 (−0.11)	−0.32 (0.32)	0.10 (−0.10)	0.26 (−0.26)	−0.41 (−0.41)	— (—)
	HOMO	0.28 (0.28)	0.25 (0.25)	−0.11 (−0.11)	−0.32 (−0.32)	−0.10 (−0.10)	0.26 (0.26)	−0.41 (−0.41)	— (—)
2	LUMO	−0.27 (0.27)	0.25 (−0.25)	0.10 (−0.09)	−0.33 (0.33)	0.09 (−0.10)	0.25 (−0.25)	−0.41 (0.41)	0.02 (−0.02)
	HOMO	0.29 (0.29)	0.25 (0.24)	−0.13 (−0.13)	−0.32 (−0.32)	−0.14 (−0.13)	0.24 (0.25)	−0.39 (−0.39)	0.06 (0.06)
3	LUMO	−0.26 (0.26)	0.25 (−0.26)	0.07 (−0.08)	−0.33 (0.33)	0.07 (−0.09)	0.26 (−0.25)	−0.41 (0.41)	0.13 (−0.13)
	HOMO	0.29 (0.29)	0.21 (0.21)	−0.18 (−0.18)	−0.29 (−0.29)	−0.18 (−0.18)	0.21 (0.21)	−0.34 (−0.34)	0.26 (0.26)
4	LUMO	0.26 (−0.26)	−0.25 (0.26)	−0.09 (0.07)	0.33 (−0.33)	−0.07 (0.09)	−0.26 (0.25)	−0.41 (0.41)	−0.13 (0.13)
	HOMO	0.29 (0.29)	0.20 (0.20)	−0.18 (−0.18)	−0.26 (−0.26)	−0.18 (−0.18)	0.20 (0.20)	−0.32 (−0.32)	0.30 (0.30)
7	LUMO	0.24 (−0.24)	−0.14 (0.14)	−0.18 (0.18)	0.21 (−0.21)	−0.17 (0.17)	−0.14 (0.14)	0.25 (−0.25)	0.32 (−0.32)
	HOMO	−0.26 (−0.26)	−0.26 (−0.26)	0.07 (0.07)	0.32 (0.32)	0.08 (0.08)	−0.25 (−0.25)	0.41 (0.41)	0.02 (0.02)
8	LUMO	0.29 (−0.29)	−0.22 (0.22)	−0.16 (0.16)	0.31 (−0.31)	−0.15 (0.15)	−0.22 (0.22)	0.36 (−0.36)	0.11 (−0.11)
	HOMO	0.27 (0.27)	0.25 (0.25)	−0.10 (0.10)	−0.32 (−0.32)	−0.11 (−0.11)	0.24 (0.24)	−0.39 (−0.39)	0.04 (0.04)
9	LUMO	−0.04 (0.32)	0.11 (−0.10)	0.01 (−0.25)	−0.11 (0.21)	0.00 (−0.25)	0.11 (−0.10)	−0.25 (0.11)	0.05 (0.52)
	HOMO	−0.40 (−0.13)	−0.22 (−0.20)	0.25 (0.02)	0.35 (0.22)	0.25 (0.03)	−0.22 (−0.20)	0.26 (0.40)	−0.35 (0.03)
10	LUMO	0.36 (−0.18)	−0.23 (0.21)	−0.21 (0.06)	0.37 (−0.25)	−0.20 (0.06)	−0.24 (0.21)	0.32 (−0.40)	0.15 (0.02)
	HOMO	0.23 (0.32)	0.24 (0.25)	−0.08 (−0.15)	−0.30 (−0.34)	−0.09 (−0.16)	0.24 (0.24)	−0.40 (−0.36)	0.03 (0.07)

Table 7 Charge distribution at ground and excited state of compound **1**—**4** and **7**—**10**

	1	**2**	**3**	**4**	**7**	**8**	**9**		**10**	
Substitute	H	CH_3	NH_2	$N(CH_3)_2$	NO_2	CN	NH_2	NO_2	CH_3	CN
q_0	0.020	0.026	−0.003	0.002	−0.232	−0.154	0.007	−0.241	0.029	−0.159
q_s	0.020	0.030	0.042	0.078	−0.273	−0.164	0.075	−0.300	0.036	−0.184
Δq	0.000	0.004	0.045	0.076	−0.041	−0.010	0.068	−0.059	0.007	−0.025

transition of $S_m \rightarrow S_n$ (S_m denotes the main middle excited state, S_n denotes the final state), the state possessing the largest transition moment is the final state, and the double wavelength of the $S_0 \rightarrow S_n$ is the TPA peak position. The results of compounds **1**—**4** and **7**—**10** are listed in Table 8 , the experimental data is in the parenthesis , and in agreement with our calculation basically.

Using the above method, the wavelength λ_{2c} of the TPA peaks of compounds **1**—**4** and **7**—**10** was obtained and listed in Table 8. And in order to explain the relationship between two-photon absorption cross-section (δ_{TPA}) and the micro structure, we devised a flow diagram (Figure 5) to show it more clear. In Figure 5, the arrow direction shows the increase of TPA cross-section δ. From Figure 5, It can be found that for D-π-D type the strength of donor $H < CH_3 < NH_2 < N(CH_3)_2$, the δ_{TPA} is **1**<**2**<**3**<**4**. For A-π-A type, the strength of acceptor $CN < NO_2$, the δ_{TPA} is **7**>**8**. For D-π-A type,

Table 8 Maximum one- and two-photon absorption for compounds **1**—**4** and **7**—**10**

Compound	λ_{1c} (λ_{1e})[a]/ nm	f	Configurations and weight	λ_{2c}(λ_{2e})[a]/nm	Configurations and weight
1	303.6 (312)[24]	1.2468	(34,0)→(35,0) 96% (31,0)→(38,0) 1%	465.0 (488)[25], (466)[21]	(34,0)→(38,0) 88% (31,0)→(39,0) 3%
2	331.9	1.3117	(40,0)→(41,0) 96% (39,0)→(44,0) 2%	445.8	(39,0)→(41,0) 85% (38,0)→(43,0) 4%
3	336.0	1.4595	(40,0)→(41,0) 94% (39,0)→(44,0) 3%	490.2	(39,0)→(41,0) 61% (40,0)→(44,0) 29%
4	341.2 (348)	1.5173	(52,0)→(53,0) 94% (51,0)→(56,0) 4%	497.2 (529)[21]	(52,0)→(56,0) 53% (51,0)→(53,0) 34%
7	344.7	1.5091	(50,0)→(51,0) 90% (47,0)→(52,0) 7%	463.6	(47,0)→(51,0) 50% (50,0)→(56,0) 35%
8	321.8	1.6612	(42,0)→(43,0) 95% (41,0)→(44,0) 3%	460.4	(41,0)→(43,0) 74% (38,0)→(44,0) 7%
9	371.5	1.2426	(45,0)→(46,0) 77% (45,0)→(47,0) 11%	500.0	(44,0)→(46,0) 43% (45,0)→(50,0) 24%
10	321.1	1.4587	(41,0)→(42,0) 95% (40,0)→(44,0) 2%	460.2	(40,0)→(42,0) 54% (39,0)→(42,0) 12%

[a] The experimental values λ_{1e} and λ_{1e} are given in parentheses.

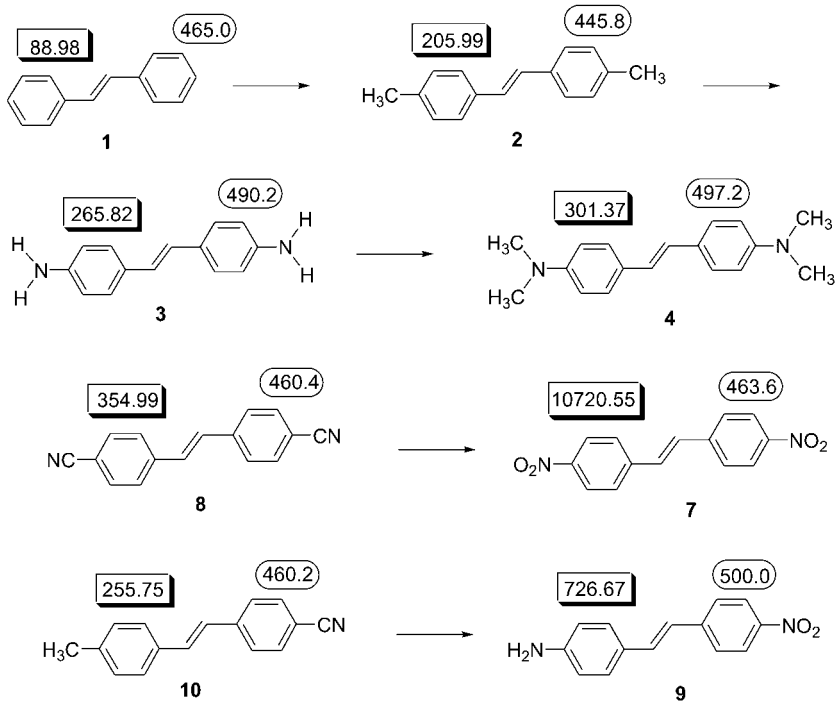

Figure 5 Flowchart of TPA cross-sections δ (ω) and TPA peaks λ_{2c} for molecules studied. Values in the rectangles represent TPA cross-sections δ (ω) [$\times 10^{-5}$ (cm^4 • s)], values in the ellipses represent TPA wavelengths λ_{2c} (nm).

the strength of donor CH_3<NH_2, the strength of acceptor CN<NO_2, the δ_{TPA} is **9**>**10**. Because of the absence for the experiment of D-π-A and A-π-A type stilbene derivatives, the conclusion above is in the scope of theoretical prediction.

In order to verify the Eq. (3), we take the molecules **1**, **2**, **8** and **10** as examples, the calculated transition dipole moments (in Debye), the vertical transition energies (in electron volt), the third-order nonlinear polarizabilities γ (included real and imaginary part) and the TPA cross-section δ are listed in Table 9. Our calculation showed that the value of $M_{01}{}^2M_{1n}{}^2/(E_{01}-E_{1n}/2)^2$ is in direct proportion to the value of $\delta(\omega)$.

Table 9 Calculated transition dipole moments (in Debye), the vertical transition energies (in electron volt) for molecules **1**, **2, 8** and **10**, the calculated third-order nonlinear polarizabilities γ (included real and imaginary part) and the TPA cross-section δ for molecules **1—4** and **7—10**

Compound	$\gamma\times10^{-34}$/esu	$\delta(\omega)\times10^{-50}$/(cm^4 • s)	M_{01}/D	M_{1n}/D	E_{01}/eV	E_{1n}/eV	$M_{01}^2M_{1n}^2\cdot(E_{01}-E_{1n}/2)^{-2}$
1	2.43+0.34i	88.98 (27.3[a], 12[b])[21]	8.96	9.75	4.08	2.67	3838.73
2	4.09+0.70i	205.99	9.32	10.04	3.74	2.78	9500.73
3	5.98+1.08i	265.82					
4	6.71+1.24i	301.37 (202.4[a], 210[b]) [21]					
7	50.83+37.07i	10720.55					
8	6.88+1.24i	354.99	9.97	12.41	3.85	2.69	11376.74
9	14.04+2.88i	726.67					
10	5.80+0.86i	255.75	9.97	11.62	3.86	2.69	9804.62

[a] From calculated value in reference [21], [b] from experimented value in reference [21].

Now, it is time for us to compare the methods of PM3 and AM1: they both can be used to optimize the geometry structure, and the calculated results are basically in agreement with the experiment, but for compounds **1—4**, the λ_{1c}(PM3) values always bigger than λ_{1c}(AM1) values, and the experimental values are between PM3 values and AM1 values. The interesting point is both PM3 and AM1 values are successively red-shifted from compounds **1** to **4**. Compared Tables 3 and 8, we found that the calculated λ_{2c} (PM3) values also always bigger than λ_{2c} (AM1) values for compounds **1—4**. Compare Tables 4 and 9, we found that the calculated δ(PM3) values always less than δ(AM1) values for compounds **1—4**.

Conclusions

Different type of stilbene including D-π-D, D-π-A and A-π-A types, all have third-order nonlinear optical properties and two-photon absorption. For each type stilbene, the higher the strength of substituents, the bigger two-photon absorption cross-section (δ_{TPA}). The geometries of molecule have some effect on the spectra, third-order nonlinear optical properties and two-photon absorption, but not too big.

References

1 Göppert-Mayer, M. *Ann. Phys.* **1931**, *9*, 273.
2 Kaiser, W.; Garrett, C. G. B. *Phys. Rev. Lett.* **1961**, 7229.
3 Bhawalkar, J. D.; He, G. S.; Prasad, P. N. *Rep. Prog. Phys.* **1996**, *59*, 1041.
4 Cumpston, B. H.; Ananthavel, S. P.; Barlow, S.; Dyer, D. L.; Ehrlich, J. E.; Erskine, L. L.; Heikal, A. A.; Kuebler, S. M.; Sandy, L. I.; McCord, M. D.; Qin, J.; Röckel, H.; Rumi, M.; Wu, X. L.; Marder, S. R.; Perry, J. W. *Nature* **1999**, *398*, 51.
5 McDonagh, A. M.; Humphrey, M. G.; Samoc, M.; Luther, D. B. *Organometallics* **1999**, *18*, 5195.
6 Chung, S. J.; Kim, K. S.; Lin, T. C.; He, G. S.; Swiatkiewicz, J.; Prasad, P. N. *J. Phys. Chem. B* **1999**, *103*, 10741.
7 Luo, Y.; Norman, P.; Macak, P.; Agren, N. *J. Phys. Chem. A* **2000**, *104*, 4718.
8 Lee, W. H.; Cho, M.; Jeon, S. J.; Cho, B. R. *J. Phys. Chem. A* **2000**, *104*, 11033.
9 Feneyrou, P.; Baldeck, P. L. *J. Phys. Chem. A* **2000**, *104*, 4764.
10 Barzoukas, M.; Blanchard, D. M. *J. Chem. Phys.* **2000**, *113*, 3951.
11 Rumi, M.; Ehrlich, J. E.; Heikal, A.A.; Perry, J. W.; Barlour, S.; Hu, Z.; McCord, M. D.; Parker, T. C.; Röckel, H.; Thayumanavan, S.; Marder, S. R.; Beljonne, D.; Brédas, J. L. *J. Am. Chem. Soc.* **2000**, *122*, 9500.
12 Pati, S. K.; Marks, T. J.; Ratner, M. A. *J. Am. Chem. Soc.* **2001**, *123*, 7287.
13 Kirkpatrick, S. M.; Naik, R. R.; Stone, M. O. *J. Phys. Chem. B* **2001**, *105*, 2867.
14 Morel, Y.; Irimia, A.; Najechalski, P.; Kervella, Y.; Stephan, O.; Baldeck, P. L. *J. Chem. Phys.* **2001**, *114*, 5391.
15 Beiljonne, D.; Bras, J. L.; Cha, M.; Torruellas, W. E.; Stegeman, G. I.; Hofstraat, J. W.; Horsthuis, H.; Lmann, G.; Perry, J. W.; Mann, S. R. *J. Chem. Phys.* **1995**, *103*, 7834.
16 Kogej, T.; Beljonne, D.; Meyers, F.; Perry, J. W.; Marder, S. R.; Brédas, J. L. *Chem. Phys. Lett.* **1998** , *298*, 1.
17 Ehrlich, J. E.; Wu, X. L.; Lee, I. Y.; Hu, Z. Y.; Rökel, H.; Marder, H. R.; Perry, J. W. *Opt. Lett.* **1997**, *22*, 1843.
18 Shen, Y. R. *The Principles of Nonlinear Optics*, Wiley, New York, **1984**.
19 Orr, B. J.; Ward, J. F. *Mol. Phys.* **1971**, *20*, 513.
20 Dirk, C. W.; Kuzyk, M. G. *Phys. Rev. B* **1990**, *41*, 1636.
21 Albota, M.; Beljonne, D.; Brédas, J. L.; Ehrlich, J. E.; Fu, J. Y.; Heikal, A. A.; Hess, S. E.; Kogej, T.; Levin, M. D.; Marder, S. R.; McCord, M. D.; Perry. J. W.; Rökel, H.; Rumi, M.; Subramaniam, G.; Webb, W. W.; Wu, X. L.; Xu, C. *Science* **1998**, *281*, 1653.
22 Ridley, J. E.; Zerner, M. C. *Theoret. Chim. Acta* **1973**, *32*, 111.
23 Molina, V.; Merchan, M.; Roos, B. O. *J. Phys. Chem. A* **1997**, 101, 3478.
24 Suzuki, H. *Bull. Chem. Soc. Jpn.* **1960**, *33*, 379.
25 Anderson, R.; Holtom, G. R.; McClain, W. M. *J. Chem. Phys.* **1979**, *70*, 4310.

(E0305064 LI, L. T.)